Consiglio Nazionale delle Ricerche

Effects of dust on start-up phase of tokamaks discharges

E. Lazzaro, M. De Angeli.

FP 2019/02 April 2019

ISTITUTO DI FISICA DEL PLASMA
"Piero Caldirola"

Via R. Cozzi 53 - 20125 Milano (Italy)

Effects of dust on start-up phase of tokamaks discharges

E. Lazzaro, M. De Angeli
Istituto di Fisica del Plasma, CNR, via Cozzi 53, 20125 Milan, Italy.

A model for gas breakdown evolution and plasma current ramp-up in tokamaks in presence of dust is presented and discussed. It is shown that the presence of dust could lead to a delay in the plasma current ramp-up up to several 100s of ms and a limitation of the current plateau value.

I. INTRODUCTION AND MOTIVATION

Dust in tokamaks is recognized to be an issue for, both, safety and operations [1, 2] issues. Recent investigations have proved the existence of magnetic dust in tokamaks [3–8] despite the fact that no magnetic material had ever been introduced in tokamaks. In fact this magnetic dust is the result of a change of the crystalline phase, from the austenite to the ferrite ones, of dust coming from non-magnetic stainless steel or inconel plasma-facing components and/or diagnostics, change caused by the extreme harsh environment present in tokamaks during operations [6]. Although the presence of dust in tokamaks has been widely investigated [9, 10], magnetic dust, on the contrary of non-magnetic one, is prone to be mobilized by the external magnetic and transformer ramp-up field *before* the beginning of plasma discharges, leading to the presence of mobilized dust in the vacuum vessel during the start-up stage of discharges. The evidence of the presence of dust in vacuum vessel during start-up has recently been documented in FTU [11] where an average dust density of $2 - 30 \times 10^{-3}$ cm^{-3} before the start-up phase was estimated. On the presence of magnetic dust and its possible impact on the discharge start-up phase in tokamaks have already been speculated in the past [3, 12]. In this report, we present a model describing the gas breakdown and plasma current ramp-up phases in presence of dust. This investigation could also be important in the perspective of using steel components and RAFM materials in ITER [13] and future fusion power plants [14, 15].

The impact on tokamaks operations of flying dust in vacuum chamber, across the plasma volume during start-up phase, could be summarized in essentially three phases, namely: i) perturbing the breakdown phase of discharges; ii) perturbing the current ramp-up phase; iii) terminating the discharge upon the full plasma is established due to the dust vaporization. In this report we focus our attention on the first two mentioned mechanisms.

II. BREAKDOWN IN PRESENCE OF TRACE DUST

To describe the breakdown phase of discharges in tokamaks and how the presence of trace dust can impact on this phase, it is instructive to start from the essential concepts of the gas discharge processes illustrated within the classical Townsend model [16]. Here we first reconsider its logic and results and extend it to the case where a very low density dust is suspended in the gas fed into the tokamak vessel before start-up. An extension of the breakdown description to suit the tokamaks conditions at start-up will be developed considering the more realistic, albeit less determined, Loeb Meek streamer breakdown model [17].

A. Classical Townsend approach

For the conceptual problem examined here, we consider a simplified 1 D steady state momentum balance and continuity equations [18] for electrons and isolated dust particles:

$$-eE - m_e\left(\nu_{en} + \nu_{ed}\right) u_e \simeq 0 \qquad (1)$$

$$u_e \frac{dN_e}{dx} = N_e(\nu_{ion} - \nu_{rec}) - N_e \overline{\nu}_{d,e} - N_e \nu_{loss} \qquad (2)$$

where m_e, u_e and N_e are, respectively, the electron mass, drift velocity, and density; E the applied electric field; ν_{en} and ν_{ed} are the electron-neutral and electron-dust collision frequencies; $\overline{\nu}_{d,e}$ is the frequency of absorption of electrons on dust; ν_{ion} and ν_{rec} are the ionization and recombination rates (ν_{rec} can be neglected in the present case); and ν_{loss} represents the electrons loss rate caused by drift effects due to the multipolar magnetic field scale length at breakdown. It should be noted that $\overline{\nu}_{d,e}$ and ν_{loss} depend on the dust density N_d, as shown in section II C. In this description, the effect of dust is to deplete the free electron available for the avalanche and it appears as a sink and friction mechanism in the above momentum and continuity equations (1) and (2). In this model, the first Townsend avalanche ionization coefficient and the electron capture coefficient are represented, respectively, by the coefficients: $\alpha\left(v\right) = N_n < \sigma_{ion} v > / u_e$ and $\beta\left(v\right) = N_d < \sigma_{e,d} v > / u_e$, where N_n is the neutral density; σ_{ion} and $\sigma_{e,d}$ are the ionization and the electron-dust impact cross sections. The frequency of absorption on dust due to the electron flux $\overline{\nu}_{d,e}$, is expressed by the relation $\overline{\nu}_{d,e} = N_d < \sigma_{e,d} v >$, as described in section II C. Estimating the electron drift velocity u_e from the momentum equation 1, with the cross sections calculated following ref.[19], it is possible deduce the expression of the two coefficients $\alpha(E, p_g) = A p_g \exp(-B p_g / E)$ and $\beta(E, N_d) \approx \overline{\nu}_{d,e}/(\mu_e E)$, where μ_e is the electron mobility [20], p_g is the gas pressure, and A and B the appropriate Paschen coefficients.

B. Loeb Meek streamer approach

In tokamaks environment of interest here, significantly different from the Townsend d.c. discharge between two electrodes, a more realistic model is perhaps that of the formation of localized 'streaming' space charge [16, 17], in a transient non-uniform applied field. In the streamer mechanism it is assumed that the growth of a single electron avalanche becomes unstable before reaching the anode. This results in the formation of fast moving *streamers*. The conditions necessary for streamer propagation, according to ref. [16] are: (i) that sufficient high energy photons must be created in the initial electron avalanche to ionize some of the gas atoms or molecules present, (ii) that these photons be absorbed to produce ions in adequate proximity to the streamer tip, and (iii) *that the space-charge field at the rear of the avalanche tip shall be of the same order of magnitude as the applied field to give adequate secondary avalanches in the enhanced field.* Meeks criterion is based on condition (iii) [16, 17]. The *standard expression* of the breakdown electric field E vs. p_g (Paschen law) is obtained from equation (2) by equating the steady state ionization rate with the effective loss rate $\alpha = 1/L_{Loss}(N_d)$, obtaining the form $E\,(p_g) = \frac{Bp_g}{ln(Ap_gL_{Loss})}$, where $L_{Loss}(N_d, \nabla B/B) = \frac{u_e}{\nu_{loss}(N_d,\nabla B/B)}$. Details on the calculation of the coefficients A and B, for a study case, can be found in section II C.

In Fig. 1 a typical plot of $E(p_g)$ is given for different lengths $L_{Loss}(N_d)$, for the typical values of the (FTU) gas filling state, polluted by trace of Fe dust particles spanning from $0.05N_d$ to $2N_d$ with $N_d = 6 \times 10^{-3}$ cm^{-3}. It is evident the dependence of the working point from the dust density concentration.

Moreover, *in presence of dust* the effective breakdown condition is given by

$$\alpha\,(E, p_g) - \beta\,(E, N_d) = 1/L_{Loss}(N_d) \qquad (3)$$

as shown in Fig.2 for a constant pressure $p_g = 5 \times 10^{-3}$ Pa and two values of dust densities and lengths $L_{Loss}(N_d)$. The intercepts with the E axis show the existence of a critical field (or loop voltage) below which the discharge does not grow in presence of dust.

C. Townsend coefficients

The two Townsend coefficients α and β can be deduced from the momentum balance equation (1) and the continuity equation (2). On the rhs of the continuity equation the processes of ionizing collision with neutrals, recombination (negligible in the present case) and attachment are represented by their rates obtained from the cross sections of the different collisional processes $\nu_{ion} = N_n < \sigma_{ion} v >$, $\nu_{rec} = N_i < \sigma_{rec} v >$, $\nu_{ed} = N_e < \sigma_{e,d} v >$. The last term in the continuity equation represents effective losses that is summarized

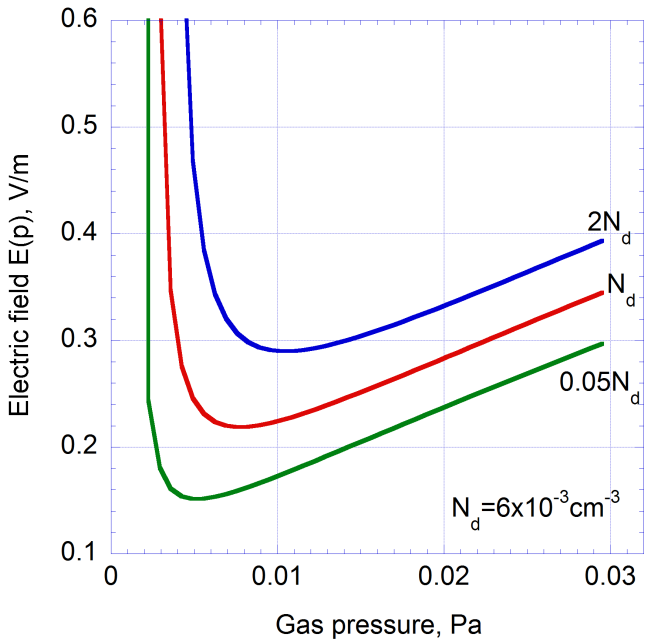

FIG. 1: Plot of the breakdown electric field E vs. p_g (Paschen law), $E(p_g) = \frac{Bp_g}{ln(Ap_gL_{Loss})}$, $A \simeq 1.91\,\mathrm{Pa}^{-1}\mathrm{m}^{-1}$, $B \simeq 25.97\,\mathrm{V\,Pa}^{-1}\mathrm{m}^{-1}$ with dust effect in connection length. The red line is the curve for $L_{Loss}(N_d) = 169$ m, with $N_d = 6 \times 10^{-3}\,\mathrm{cm}^{-3}$; the blue line for $2N_d$, $L_{Loss}(2N_d) = 127.5$ m; and the green line is the curve for $0.05N_d$, $L_{Loss}(0.05N_d) = 244$ m. Other experimental parameters assumed: filling gas D_2, $p_g = 5 \times 10^{-3}$ Pa, $r_d = 100$ μm.

in the electron loss rate $\nu_{loss} \approx u_e/L_{Loss}$ which depends on the effect of electrons drifts in the multipolar $\mathbf{B}$ field present before the plasma current builds up and on the electron free flight between two capture collisions with dust, $\ell_{ed}(N_d) \approx \frac{u_e}{\nu_{ed}} \propto \frac{\mu_e E_0}{r_d^2 v_{the} N_d}$ with μ_e the electron mobility and v_{the} the thermal electron velocity. Then L_{Loss} is defined as $L_{Loss} = \frac{L_q}{1+L_q/\ell_{ed}}$ which interpolates from vanishing N_d to large N_d and L_q is the effective magnetic connection length which is several torus $2\pi R_0$ circumferences.

In fact, before a plasma current is formed, the magnetic field consists of externally applied toroidal and multipolar components: $\mathbf{B} = \mathbf{B}_\phi + \mathbf{B_m}$. The multipolar field must have a sufficiently high order null on the axis where the current channel formation is desired. In the present case, in the (R, ϕ, Z) coordinate frame, with $\rho = R - R_0$, $\theta = \tan^{-1}\frac{Z}{R-R_0}$ we consider an hexapolar field $\mathbf{B_m} = \mathbf{B_{hex}} = \mathbf{B_0}\frac{\rho^2}{\mathbf{a^2}}(\cos(\mathbf{2}\theta)\mathbf{e_R} - \sin(\mathbf{2}\theta)\mathbf{e_Z})$, where R_0 and a are major and minor radius of the tokamak. The initial formation of a current channel of radius $\approx \rho$, occurs when the pinch effect overcomes the tearing force due to the external (multipolar) field B_m, $\mathbf{J} \times \mathbf{B} \geq \mathbf{J} \times \mathbf{B_m}$. In order of magnitude this condition is $I \geq 5 \times 10^6 \rho B_m$ in MKS units. By surface averaging over an area $S = \pi\rho^2 < \pi a^2$ surrounding the null point,

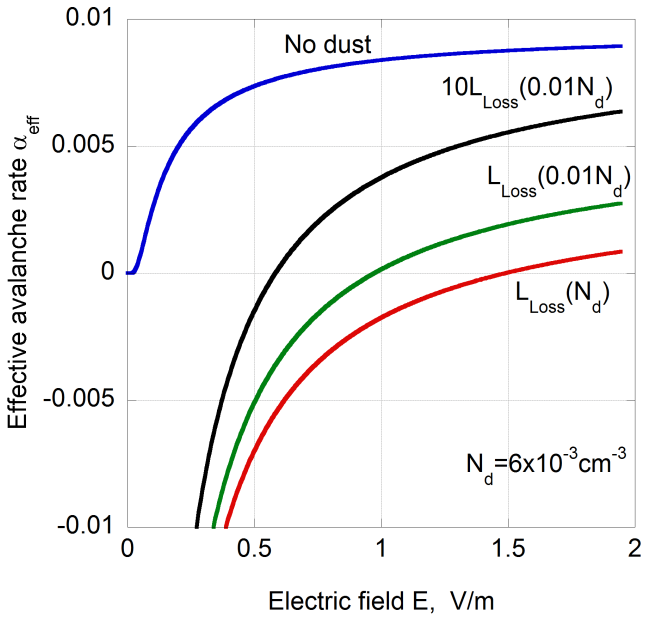

FIG. 2: Plots of the effective avalanche rate $\alpha_{eff} = \alpha - \beta - 1/L_{Loss}$ vs. E at constant p_g. The blue line plot is $\alpha(E, p_g)$ *without dust effect*; the red line is for the effective rate with $L_{Loss}(N_d) = 169$ m, $N_d = 6 \times 10^{-3}\,\mathrm{cm}^{-3}$; the green line for $L_{Loss}(0.01N_d) = 249$ m; and the black line is for $10L_{Loss}(0.01N_d) = 2490$ m. The intercept gives the critical E value for breakdown.

an estimate of the effective L_q length is $L_q \approx 4\frac{B_\phi}{<|\nabla B_{hex}|>}$.

The first Townsend avalanche ionization coefficient is represented by $\alpha\,(v) = N_n < \sigma_{ion} v > /u_e$. The parallel electron drift velocity is obtained from the momentum equation $u_e \simeq \left(\frac{-e}{m_e \nu_{en}}\right) E = \mu_e E \propto \frac{E}{p_g}$, where p_g is the neutral gas pressure. The coefficient α is related to the mean free path (λ) and the ionization length (λ_I) by the relation $\alpha = \frac{e^{-\lambda_I/\lambda}}{\lambda} \sim \frac{\sigma_{ion} p_g}{k_B T_g}$ where $\lambda_I = 13.6$ eV/eE. Due to the dominant collisions with neutrals the direct influence of dust on λ can be neglected. For the integrated ionization cross section we apply strictly the full expression of the advanced BEQ (modified Binary Encounter Bethe) model [19], obtaining $\sigma_{ion} = \sigma_{I-BEQ}(10eV) = 7.2{\times}10^{-21}\,\mathrm{m}^2$. As a case study we consider the gas pressure $p_g = 5 \times 10^{-3}$ Pa and the temperature $T_g \simeq 300°\mathrm{K} \approx 0.0258$ eV. Eventually α is expressed as $\alpha(E, p_g) = A p_g \exp(-B p_g/E)$; here $A \simeq 1.91\,\mathrm{Pa}^{-1}\mathrm{m}^{-1}$ and $B \simeq 25.97\,\mathrm{V\,Pa}^{-1}\mathrm{m}^{-1}$.

The electron capture coefficient β is related to the frequency of electron absorption on dust given by the electron flux. This can be expressed, as a lower estimate, from the relation, valid in the OML framework [21], $\overline{\nu}_{d,e} = N_d < \sigma_{e,d} v > = \sqrt{8\pi} r_d^2 N_d v_{th_e} e^{Z_1}$, where $Z_1 = \frac{e^2 Z_d}{r_d T_e}$ and $Z_d \sim 10^5$ is the dust particle charge number determined by the basic static charge balance equation [21, 22], and consequently the electron capture coefficient is $\beta = N_d < \sigma_{e,d} v > /u_e \approx \overline{\nu}_{d,e}(N_d)/\mu_e E$. In the early stages of the ionization process, it is likely that the ion temperature be close to that of the prefilling gas $T_i \approx T_g \sim 0.0258$ eV. However the sensitivity to $\tau = T_i/T_e$ is modest and, for *a particular example*, it is convenient to consider $T_e = 1$ eV, $\tau = 1$, $N_d \approx 6 \times 10^{-3}\,\mathrm{cm}^{-3}$, $N_e \simeq N_i \approx 1.24 \times 10^{12}\,\mathrm{cm}^{-3}$, $r_d = 100\,\mu$m, $\nu_{ed} \approx 7.32\,\mathrm{s}^{-1}$.

III. CURRENT RAMP-UP AND TRANSITION TO INDUCTIVE DISCHARGE

The basic physical problem concerning the transformation from the avalanche discharge to the inductive current rise, consists in determining the time constant of the transformation and of the corresponding typical value of the current and its scaling with the main parameters of the early discharge state [23]. These parameters depend on the condition of the avalanche (Pedersen-Meek condition) and on the discharge resistance which is affected by the impurity content. The mechanisms retarding or inhibiting the discharge are to be sought in the breakdown time constant, which depends not on the impurity densities but on the electron "attachment" rate to dust being an "extraneous body". In the Meek-Pedersen avalanche process the current grows exponentially as $I_{av}(t) = I_0(e^{\frac{t}{\tau_b}} - 1)$, where the effective avalanche rate is $\tau_b^{-1} = (\alpha(N_d) - \beta(N_d))u_e$. The relation between the current and the voltage is resistive at the very early stages of the discharge. As the discharge proceeds the plasma current is limited by the self-inductance. In a lumped parameters description, the evolution of the plasma current I is governed by the circuit equation for the plasma loop, inductively coupled to the transformer primary circuit. Here we refer in the following to a basic scheme of inductive storage and primary transformer circuit, shown and described in the caption of Fig.3. The rise of the current depends on the type of applied loop voltage waveform, ranging from simple primary circuit breaking to feedback control of the current or the rate of rise: the different operation leads to different matching conditions with the initial, "spontaneous" avalanche phase. The aim of this paragraph is to discuss the matching of the two phases, i.e. the avalanche discharge followed by the inductively current rise phase, and establish if the presence of dust can *significantly* delay the beginning of the inductive phase and/or limit the plasma current at plateau.

The plasma current evolution in the inductive phase can be described by a single, lumped parameters, nonlinear equation

$$\frac{dI_{ind}}{dt} + \frac{R_p(I_{ind})}{L} I_{ind} = \frac{V(t)}{L} \qquad (4)$$

where L is the discharge self-inductance and $R_p = R_p(Z_{eff}, I_{ind})$ the plasma resistance associated with a matching condition with the avalanche current $I_{av}(t)$ at some time $t = t_m$. The avalanche value of the current

can be estimated adapting the Townsend model [16], indicated as I_0.

An illustration of the time behavior of the current in the breakdown and inductive phase for the parameters considered here is described in the following sections.

A. Nonlinear Circuit Equation

To gain physical insight of the inductively discharge phase it is useful to consider the current circuit coupled to an (0D) energy equation. The plasma resistivity depends on the temperature T and the effective Z_{eff} of the plasma by the relation $\eta \propto Z_{eff} ln\Lambda T^{-3/2}$ and can be represented by $\eta_0 \big(\frac{T_0}{T}\big)^{\frac{3}{2}}$. The simplified energy balance with Ohmic heating input and lumped effective loss, reads:

$$L\frac{dI}{dt} + R_{p0}(Z_{eff})\big(\frac{T_0}{T}\big)^{\frac{3}{2}} I = V\big(t\big) \tag{5}$$

$$\frac{dNT}{dt} = \eta_0 \big(\frac{T_0}{T}\big)^{\frac{3}{2}} \frac{I^2}{S^2} - \frac{NT}{\tau_E} \tag{6}$$

where L and S are the (a priori) varying discharge self-inductance and cross section, and τ_E is an effective energy loss (confinement) time for the early plasma condition, which in the stage of current pinch development cannot be longer than the (single) particles confinement time, therefore of the order of the drift time in the multipolar field. A dimensional argument applied to the energy balance equation leads to the scaling of the discharge temperature with current (assuming, tentatively on a short time interval after breakdown, constant density and cross section):

$$\big(\frac{T_0}{T}\big)^{\frac{3}{2}} = (\frac{NT_0}{\tau_E})^{\frac{3}{5}} (\frac{S^2}{\eta_0})^{\frac{3}{5}} I^{-\frac{6}{5}} \equiv I_{T_0}^{\frac{6}{5}} I^{-\frac{6}{5}} \tag{7}$$

where $I_{T_0} = \big(\frac{N_{e0} T_{e0}}{\eta_0 \tau_E}\big)^{1/2} S$, built on reference plasma values, is a scaling parameter which *must* be considered adjustable, within bounds discussed below, given the uncertainty of the early discharge cross section S and energy confinement time. Consequently $R_p = R_{p0}(\frac{T_{e0}}{T_e})^{\frac{3}{2}}$ is a function of $(\frac{I_{T_0}}{I})^{\frac{6}{5}}$, which for numerical evaluation is conveniently expressed by the smooth transition expression $R_p = R_{p0}\left(1 + (\frac{I}{I_{T_0}})^{\frac{6}{5}}\right)^{-1}$. The inductive-resistive stage of the current evolution is then governed by the single nonlinear equation

$$\frac{dI}{dt} + \frac{R_{p0}}{L} \frac{I}{1 + (\frac{I}{I_{T_0}})^{\frac{6}{5}}} = \frac{V\big(t\big)}{L} \tag{8}$$

The self consistent expression of the resistance limits the influence of errors and uncertainties of other quantities, such as T, N, S, τ_E confining them in a single *fitting* parameter I_{T0}. The effect of the Meek-Townsend avalanche process is contained in the breakdown time scale τ_b and in the delay time scale t_m to be determined. The first avalanche stage is followed, after the matching time t_m, by the nonlinear inductive current rise with a possible reduction of the current plateau value. It should be noticed that an increase of dust density could be sufficient to quench the start-up. In this stage, where T_e is constant and very low, a perturbation of plasma resistivity due to the presence of dust atoms can be estimated from the amount of impurity atoms vaporized by plasma. The total Fe atoms carried by magnetic dust of $50 - 1000\,\mu$m of diameter with a density of $N_d \approx 10^{-3}\,\text{grains/cm}^3$ is about $10^{12} - 10^{16}\,\text{at/cm}^3$. If only 1% of the total dust material is vaporized by plasma heat load, the impurity concentration become comparable to the plasma density leading to a rising of Z_{eff} and to the plasma resistivity. An increase of resistivity actually accelerates the transformer driven electric field penetration, but the consumption of the stored magnetic flux is mainly resistive leading to a possible decrease of the plateau current.

B. Linear approach

The evolution of the plasma current starting from the breakdown process is a problem of matching the inductive stage with the avalanche one at some time point. The matching conditions represent different choices in the tokamak operation. To gain insight it is useful to address first the linear version of eq.8, which, associated with a sufficiently realistic waveform of the loop voltage, has an exact solution. Consider the model waveform and the linear circuit equation (see Fig.4) :

$$V(t) = V_0[e^{-t/\tau_v} + \phi_0] \tag{9}$$

$$\frac{dI}{dt} = -\frac{I(t)}{\tau_R} + \frac{V\big(t\big)}{L} \tag{10}$$

It is convenient to use the notation $U_0 = V_0/L$, $\tau_R = L/R_{p0}$, $\gamma = 1/\tau_R$, $\gamma_b = 1/\tau_b$, $\gamma_v = 1/\tau_v$, $V_0\phi_0 = V_\infty = R_0 I_\infty$; eq.9 can be rewritten as

$$U(t) = U_0 e^{-\gamma_v t} + \gamma I_\infty. \tag{11}$$

The formal solution of eq.10, the inductive current, and of the avalanche current are

$$I_{ind}(t) = Be^{-\gamma(t-t_m)} + \frac{U_0\phi_0}{\gamma}(1 - e^{-\gamma(t-t_m)}) \tag{12}$$

$$+\frac{U_0 e^{-\gamma_v t_m}}{\gamma_v - \gamma}\big[e^{-\gamma(t-t_m)} - e^{-\gamma_v(t-t_m)}\big] \tag{13}$$

$$I_{av}(t) = A\big[e^{\gamma_b t} - 1\big] \tag{14}$$

where t_m is the time of matching of the two currents (12) and (14). Let us study now what would be the behavior of the beginning of the current evolution in absence of dust (i.e. in case of a pure inductive discharge), $t_m = 0$ and $\gamma t << 1$:

$$I_{ind}(t) \simeq \frac{U_0}{\gamma_v - \gamma}\big[e^{-\gamma t} - e^{-\gamma_v t}\big]. \tag{15}$$

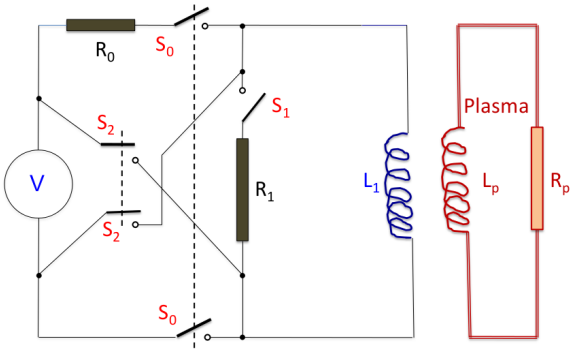

FIG. 3: Schematic pulsed transformer circuit coupled to plasma. R_0 and S_0 are the primary resistor and make switch charging primary (transformer) inductor L_1; R_1 and S_1 are the primary crowbar resistor and break switch discharging primary inductor on a time scale $\tau_v \simeq L_1/R_1$ and driving inductively the current in the plasma (secondary); at $t_s \sim 5-6\tau_v$, S_2 are closed after breaking S_0, thereby reversing the current ramp of the generator through the inductance L_1, driving a low, constant V_{loop} for the plasma flat top (see Fig.4).

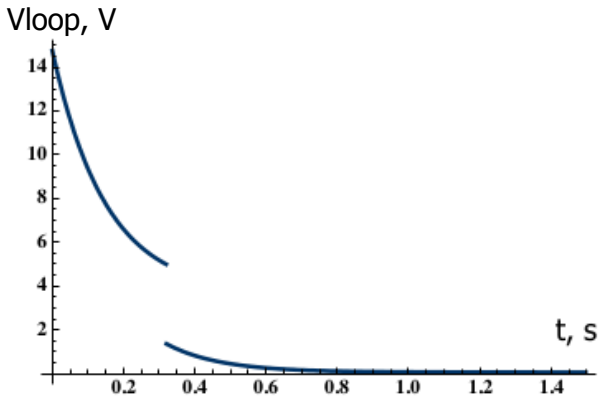

FIG. 4: Plot of applied loop voltage model waveform $V(t) = V_0(e^{-\gamma_v t} + \phi_0 H(t-t_s))$, $[V]$, where t_s is a switching time. The data are close to those of an actual FTU experiment: at $t_s = 0.3$ s the voltage is switched to a low value for the flat top phase of the plasma current.

This expression, for a purely inductive discharge, would grow from zero to a value eventually matching the avalanche value. Imposing a certain current rate U_0 leads to match the two expressions of the current at some time t_m.

$$I_{ind}(t_m) = I_{av}(t_m) \tag{16}$$

$$\frac{U_0}{\gamma_v - \gamma}\left[e^{-\gamma t_m} - e^{-\gamma_v t_m}\right] = A\left[e^{\gamma_b t_m} - 1\right] \tag{17}$$

After the breakdown delay, the current ramps up with the rate prescribed by U_0, possibly within a feedback loop not considered now.

Another interesting scenario results in the delay of the discharge ramp-up and reduction of the flat top, when no loop voltage control is applied. The current evolution described by eq.12 in this case is associated with the conditions of smooth matching of the current and its derivative:

$$I_{ind}(t_m) = I_{av}(t_m) \tag{18}$$

$$\frac{dI_{ind}}{dt} = \frac{dI_{av}}{dt} \tag{19}$$

the explicit conditions give:

$$B = A[e^{\gamma_b t_m} - 1] \tag{20}$$

$$-B\gamma + U_0[e^{-\gamma_v t_m} + \phi_0] = A\gamma_b e^{\gamma_b t_m} \tag{21}$$

the exactly matched solution is shown in Fig.5, for the loop voltage waveform of Fig.4.

C. Nonlinear approach

For the nonlinear case the approach can be of retaining similar matching conditions. In the first case of sharp matching of the avalanche current with the inductive one, equation 17 applies to the linearized version at $t < t_m$, and after t_m the current ramp is described by the numerical solution of eq.8, with the nonlinear resistance shown in Fig.6. The nonlinear solution for this scenario is shown in Fig.7. For the case of smooth matching corresponding to the exact solution of eq.12 of the linear problem it is convenient to introduce the notation $z = e^{\gamma_b t_m} \geq 1$ and $g = z/(z-1)$; from the matching conditions and for simplicity, replacing $U_0[e^{-\gamma_v t_m} + \phi_0]$ with a constant $\overline{U}_0$, formal nonlinear algebraic expressions are obtained for g, with $I(t_m) = I_0$, the Townsend avalanche current [16]. Expressing in terms of $B = I_0$, with $\overline{\gamma} = \frac{1}{\tau_R}\left[\frac{I_{T_0}}{I_0}\right]^{6/5}$:

$$B = A[z-1] \tag{22}$$

$$-B\overline{\gamma} + \overline{U}_0 = A\gamma_b z \tag{23}$$

by eliminating A between these two conditions one gets:

$$-B\overline{\gamma} + \overline{U}_0 = B\gamma_b g \tag{24}$$

$$\Rightarrow g = -\frac{\overline{\gamma}}{\gamma_b} + \frac{\overline{U}_0}{B\gamma_b} \tag{25}$$

which eventually is translated into the physical variables:

$$g = \frac{\overline{V}_0\tau_b}{LI_0} - \frac{\tau_b}{\tau_R}\left[\frac{I_{T_0}}{I_0}\right]^{6/5} \tag{26}$$

The dependence of the matching time t_m on the main physical parameters is then expressed, to leading order in γ_v and with some rearrangement, as:

$$t_m = \tau_b ln[(C_V\frac{\tau_R}{\tau_b} - C_I)] - ln[(C_V\frac{\tau_R}{\tau_b} - C_I - \frac{\tau_R}{\tau_b}] \tag{27}$$

However it must be noted that actually $C_V = \frac{\overline{V}_0\tau_b}{LI_0}$, $C_I = \left[\frac{I_{T_0}}{I_0}\right]^{6/5}$ are *constants* which for purposes of modelling,

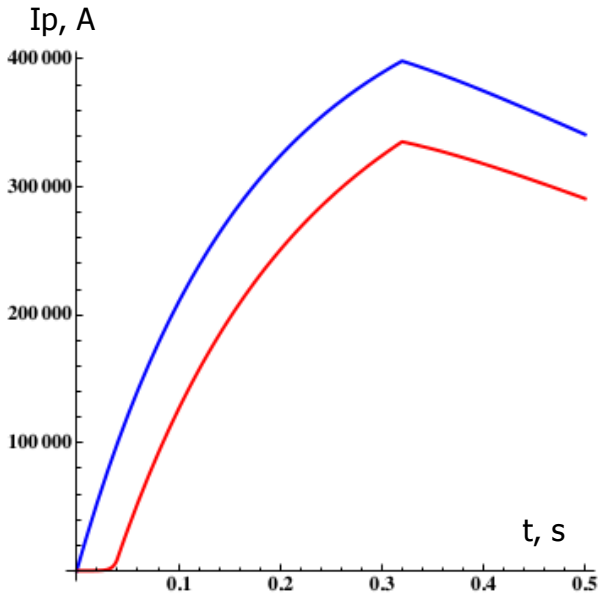

FIG. 5: Plot of plasma current build-up in linear model: $I(t)$ evolution through the breakdown phase to the inductive one, with fixed resistance. The red line shows the exact match from the low level of the early Townsend avalanche stage $I_{av}(t)$ to the much faster inductive one, with Fe dust at a density of $N_d = 6 \times 10^{-3}\,\mathrm{cm}^{-3}$. The blue line is for the case with no dust. In this example, for simplicity, the flat top of the current is not sustained by the loop voltage.

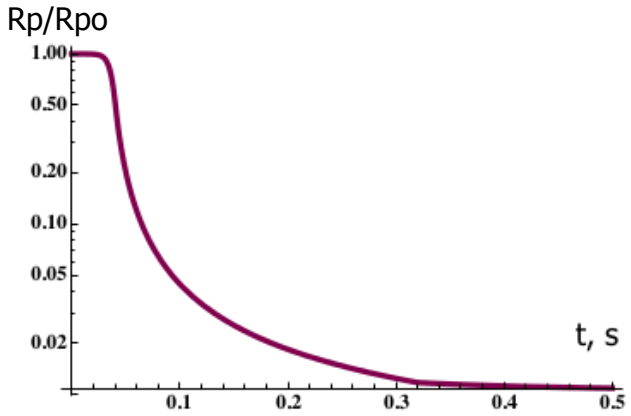

FIG. 6: Plot of time evolution of self consistent normalized resistance, with data of Fig. 4.

should be considered as adjustable parameters, given the uncertainties of the values of $I_0, I_{T_0}, \overline{V}_0, L, \tau_R, \tau_b$. Therefore the matching time t_m is generically a multiple K of the breakdown time τ_b. The effect of the nonlinearly varying resistance (Fig. 6) is apparent from Fig.8 which shows the difference between the linear and nonlinear model, in the case without dust. The nonlinear solution

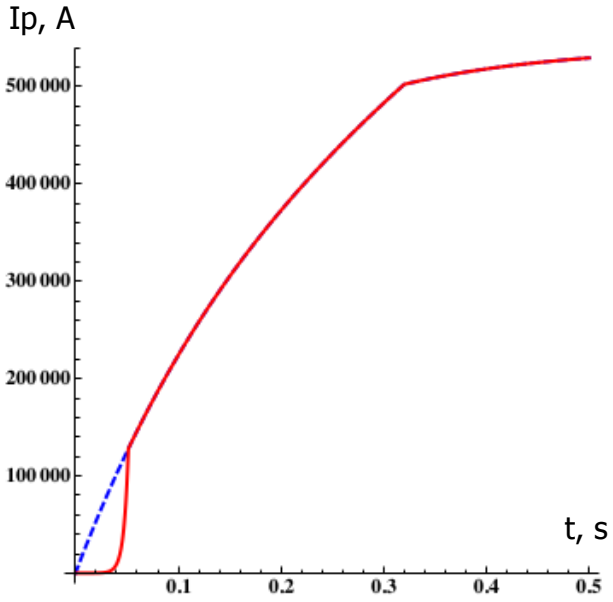

FIG. 7: Plot of plasma current build-up with the non linear model: $I(t)$ with sharp transition through the breakdown phase to the inductive one, with thermally evolving resistance. The red line shows the transition from the low level of the early Townsend avalanche stage $I_{av}(t)$ to the much faster inductive one, with Fe dust density $N_d = 6 \times 10^{-3}\,\mathrm{cm}^{-3}$. The blue dashed line is for the case with no dust.

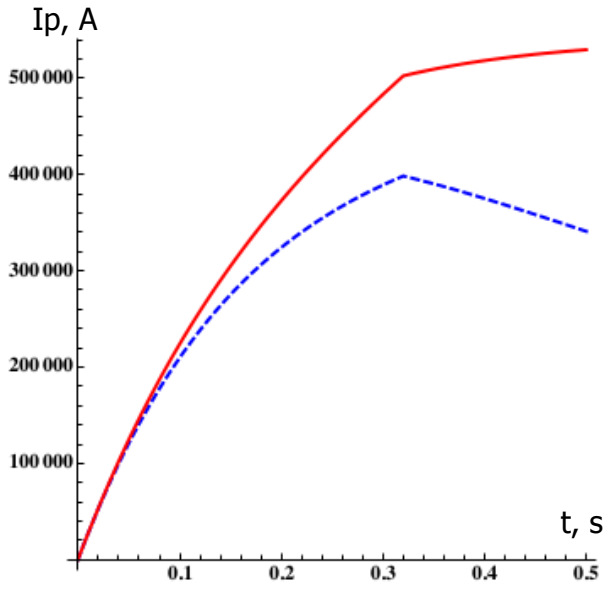

FIG. 8: Comparison of plasma current build-up in linear and nonlinear models, in absence of dust effect: the blue dashed line is for the linear case and the red one for the nonlinear one, with consistently evolving resistance.

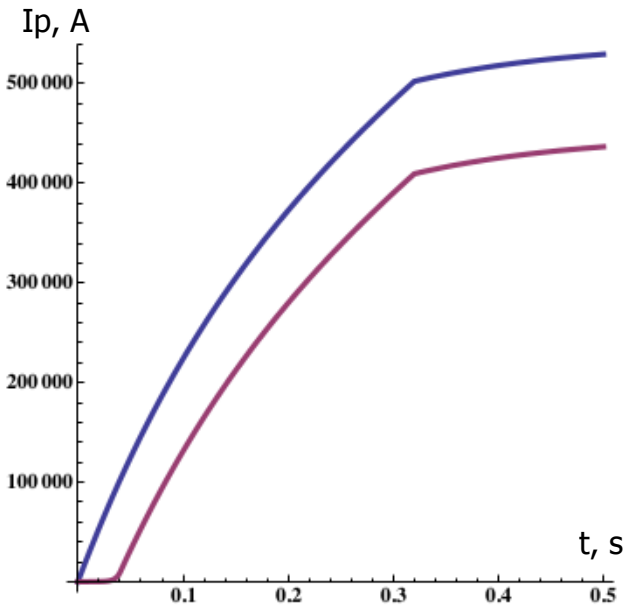

FIG. 9: Plot of plasma current build-up with the non linear model: $I(t)$ with smooth transition through the breakdown phase to the inductive one, with thermally evolving resistance. The blue line is for the case with no dust. The red line shows the transition from the low level of the early Townsend avalanche stage $I_{av}(t)$ to the much faster inductive one, with Fe dust density $N_d = 6 \times 10^{-3}\,\mathrm{cm}^{-3}$.

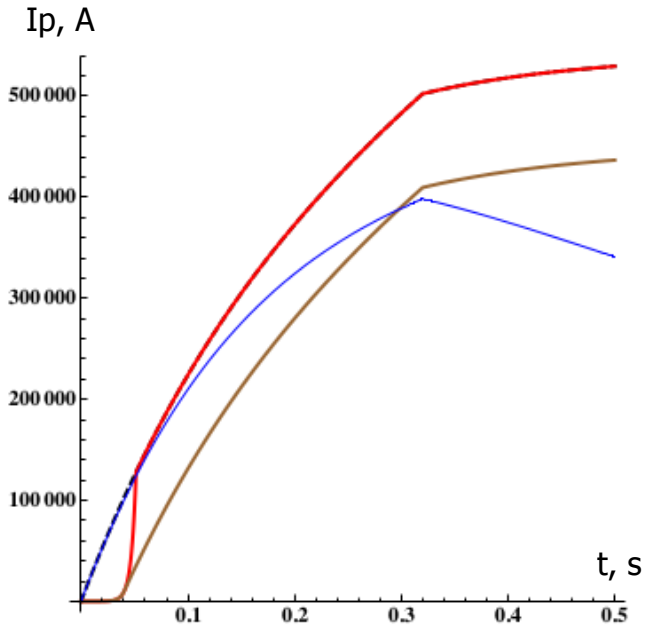

FIG. 10: Comparison of current build-up for three models: the dashed black line is the case with no dust; the red line is the case with dust and sharp transition from avalanche to inductive phase; the brown line is the case with dust and smooth transition from avalanche to inductive phase; the blue line is the linear case without dust.

for this scenario is shown in Fig.9. A solution of the nonlinear problem can be also obtained requiring the matching of the derivatives (eq.23) and constructing an asymptotically composite solution $I(t) = I_{av}(t)H(t_m - t) + I_{ind}(t)H(t-t_m) - \left[I_{ind}(t_m) - I_{av}(t_m)\right](t)H(t_m - t)$, where H(x) is the Heaviside step function, equal to one for positive argument. The matching time is obtained evaluating numerically dI_{ind}/dt from eq.8 integrated from t=0 and intersecting it with the r.h.s of eq.23. A comparison of the three current build-up models is shown in Fig.10. The behaviour displayed by this model (Figs.7,9) has strong similarity with the experimental cases of *driven* recovery of the discharge after a hesitation, normally due to difficulties in "burn-through", associated to massive presence of light impurities. In the present case the hesitation and delay in take-off is predicted to be due to a *totally different mechanism*: the subtraction of avalanche electrons by a sufficient density of dust particles as they charge up [21] .

IV. SUMMARY OF THEORETICAL RESULTS

The above theoretical results describe the mechanisms that could interfere with the early stages of the plasma pulse build-up as a consequence of the presence of magnetic dust mobilized prior to the plasma discharge. The above mechanisms can be summarized as follows.

Breakdown phase. The reduction of the effective avalanche rate due to electron attachment to dust can induce a shift of the Paschen's curve, changing the conditions for gas breakdown. A severe reduction of the effective avalanche rate could result in a delay, up to few 100s ms, in the plasma current ramp-up phase.

Plasma resistivity. Dust can increase Z_{eff}, by the release of impurities (Fe). In the flat-top stage where I and T are practically constant, the behaviour is again linear, and for a given loop voltage the at top current is reduced by an increase of $R_p \propto Z_{eff}$.

The significance of the impact of the presence of such mobilized dust on tokamaks operations depends of course on the actual amount of dust presents in each single discharge. However the novel mechanism discussed here, due to dust, could be useful for interpreting some unclear phenomena observed at start-up phase in tokamaks, generally associated with intense impurity radiation and difficulties in reaching the discharges ignition. It should also mentioned that the above discussion and results do not aim modelling any specific experimental discharge but, more generally, are meant to be a pure elaboration of the plasma breakdown and ramp-up theory. In particular, the initial delay of discharges ramp-up is caused by a depleting of electrons in the avalanche phase that, in this case, is due to the presence of dust but, more generally speaking, could be due to any phenomenon leading to loss of available electrons. In actual tokamaks discharges many factors play a role in the build-up of the plasma current, which have not been considered in this work. In

fact this analysis has just the aim to draw the attention of readers on possible impact of dust, mobilized before a plasma discharge, on the positive evolution of discharges.

V. CONCLUSIONS

In this report we have presented a model to discuss the breakdown and ramp-up phase of tokamak discharge in presence of dust. This study shows that the possible presence of magnetic dust in future devices should be considered. In fact, as well known, ITER [24] and future plants [25] will be equipped with superconductive coils that require low loop voltage for plasma breakdown and start-up. As discussed in this paper, the presence of dust during breakdown and start-up phases of plasma discharges could require larger loop voltage for the plasma breakdown, in contrast to technical constraints for these devices.

Acknowledgments

Authors acknowledges G. Granucci and D. Ricci for valuable discussion.

[1] J. P. Sharpe, D. A. Petti and H.-W. Bartels, *Fusion Eng. Des.* **63-64** (2002) 153.
[2] J. Roth, E. Tsitrone, A. Loarte, Th. Loarer, G. Counsell, R. Neu, V. Philipps, S. Brezinsek, M. Lehnen, P. Coad, Ch. Grisolia, K. Schmid, K. Krieger, A. Kallenbach, B. Lipschultz, R. Doerner, R. Causey, V. Alimov, W. Shu, O. Ogorodnikova, A. Kirschner, G. Federici, A. Kukushkin, EFDA PWI Task Force, ITER PWI Team, Fusion for Energy, ITPA SOL/DIV, *J. Nucl. Mater.* **390-391** (2009) 1.
[3] J. Winter, *Plasma Phys. Control. Fusion* **40** (1998) 1201.
[4] D. Ivanova, M. Rubel, V. Philipps, M. Freisinger, Z. Huang, H. Penkalla, B. Schweer, G. Sergienko, P. Sundelin and E. Wessel, *Phys. Scr.* **T138** (2009) 014025.
[5] A. N. Novokhatsky, A. E. Gorodetsky, V. K. Gusev, A. P. Zakharov and R. Kh. Zalavutdinov, *Proc. 38th EPS Conference on Plasma Physics, 27 June-1 July 2011, Strasbourg, France* **Vol. 35G** P5.066.
[6] M. De Angeli, L. Laguardia, G. Maddaluno, E. Perelli Cippo, D. Ripamonti, M.L. Apicella, C Bressan, R. Caniello, C. Conti, F. Ghezzi, G. Grosso and G. Mazzitelli, *Nucl. Fusion* **55** (2015) 123005.
[7] D. L. Rudakov, University of California, San Diego, USA, *Private communication.*
[8] C. Arnas, CNRS, Aix-Marseille Univ., PIIM, France *Private communication.*
[9] J. Winter, *Plasma Phys. Control. Fusion* **46** (2004) B583.
[10] S. I. Krasheninnikov, R. D. Smirnov and D. L. Rudakov, *Plasma Phys. Control. Fusion* **53** (2011) 083001.
[11] M. De Angeli, E. Lazzaro, P. Tolias, S. Ratynskaia, et al. *Nucl. Fusion* (2019), submitted.
[12] J. Winter, *Phys. Plasmas* **7** (2000) 3862.
[13] R. A. Pitts, B. Bazylev, J. Linke, I. Landman, M. Lehnen, D. Loesser, Th. Loewenhoff, M. Merola, R. Roccella, G. Saibene, M. Smith and V. S. Udintsev, *J. Nucl. Mater.* **463** (2015) 748.
[14] J. Roth, K. Sugiyama, V. Alimov, T. Höschen, M. Baldwin and R. Doerner, *J. Nucl. Mater.* **454** (2014) 1.
[15] K. Sugiyama, K. Schmid and W. Jacob, *Nucl. Mater. Energy* **8** (2016) 1.
[16] A. Pedersen, *I E E E Transactions on Power Systems* **86**(2) (1967) 200.
[17] L.B. Loeb, J.M. Meek, *The Mechanism of the Electric Spark* Stanford University Press 1941.
[18] U. de Angelis, G. Regnoli, S. Ratynskaia, *Phys. of Plasmas* **17** (2010) 043702.
[19] Yong-Ki Kim, Karl K. Irikura, *Electron-impact ionization cross-sections for polyatomic molecules, radicals, and ions* in: K.A. Berrington, K.L. Bell (Eds.), Atomic and Molecular Data and Their Applications, vol. CP543, American Institute of Physics, 2000, 1-56396-971-8.
[20] V. E. Golant, A. P. Zhilinsky, I. E. Sakharov, 1977 *Fundamentals of plasma physics* (New York: Wiley ed.).
[21] P. Tolias, S. Ratynskaia, U. de Angelis, *Phys. of Plasmas* **18** (2011) 073705.
[22] Havnes O.,Aanesen T. K.,Melandso F. J.Geophys. Res. **95** (1990) 6581-5.
[23] K. Hirano, *Plasma Phys.* **16** (1974) 1005.
[24] A.C.C. Sips, T.A. Casper, E.J. Doyle, G. Giruzzi, Y. Gribov, J. Hobirk, G.M.D. Hogeweij, L.D. Horton, A.E. Hubbard, I. Hutchinson, S. Ide, A. Isayama, F. Imbeaux, G.L. Jackson, Y. Kamada, C. Kessel, F. Kochl, P. Lomas, X. Litaudon, T.C. Luce, E. Marmar, M. Mattei, I. Nunes, N. Oyama, V. Parail, A. Portone, G. Saibene, R. Sartori, J.K. Stober, T. Suzuki, S.M. Wolfe, the C-Mod team, the ASDEX Upgrade Team, the DIII-D team and JET EFDA Contributors, *Nucl. Fusion* **49** (2009) 073011.
[25] H. Zohm, C. Angioni, E. Fable, G. Federici, G. Gantenbein, T. Hartmann, K. Lackner, E. Poli, L. Porte, O. Sauter, G. Tardini, D. Ward, M. Wischmeier, *Nucl. Fusion* **53** (2013) 073019.